ELSEVIER

Journal of Power Sources 80 (1999) 149–155

JOURNAL OF POWER SOURCES

Electrode compositions for carbon power supercapacitors

L. Bonnefoi [a], P. Simon [a,*], J.F. Fauvarque [a], C. Sarrazin [b], J.F. Sarrau [b], A. Dugast [a]

[a] *CNAM-Laboratoire d'Electrochimie Industrielle, 2, rue conté, 75003 Paris, France*
[b] *EXIDE-CEAC, Departement Recherche, 5-7, allies des Pierres Mayettes, 92636 Gennevillier, cedex France*

Received 18 November 1998; accepted 15 December 1998

Abstract

The purpose of this work was to prepare economically-large electrodes in order to assemble mono-element supercapacitors with a capacity of more than 300 F and to reach powers in the range of 125 W (2 V/element) with the selected structure. In this paper, results are presented from different binder compositions—PTFE and a mixture of CMC/PTFE—that were tested in order to increase the volumetric capacitance of the electrode. The electrode composition was adapted to each binder composition used. For cost reasons, the amount of PTFE was reduced and the mixture of CMC/PTFE was examined as a cheaper alternative. We have obtained more than 25 F cm^{-3} per electrode, with a time constant close to 3 s, and power outputs compatible with automotive applications.

Keywords: Supercapacitors; Applications/electric vehicles

1. Introduction

Supercapacitors were invented in order to serve several specific applications with requirements intermediate between those of rechargeable batteries and capacitors [1,2]. The main interest of these products is their capability to deliver high specific peak power, associated with a good specific energy. Three types of supercapacitors are described in the literature, using metal oxide [3], conducting polymers [4], or activated carbon [5] as active materials. Metal oxide supercapacitors provide the highest specific peak power (> 5 kW kg^{-1}), but the high cost of the active material (RuO_2) makes it too expensive for some applications. Conducting polymer-based supercapacitors can reach specific power values of approximately 2 kW kg^{-1} with a specific energy of more than 10 W h kg^{-1}. But up to now, this technology is less developed industrially than the others. Specific power delivered by carbon/carbon supercapacitors can reach 3 kW kg^{-1}, with maximum specific energies of 5 W h kg^{-1}. In this latter type, the cost of the active materials (high-surface activated carbons) is very cheap. This makes this type of supercapacitor interesting for many applications, such as mobile telecommunications, back-up power for engine starting, etc. [6,7].

Carbon/carbon supercapacitors also called Double Layer Capacitors (DLC), function on the basis of the Helmholtz double layer. There is no charge transfer, as the energy is stored in the double layer near the carbon surface. The use of an organic electrolyte allows a voltage of 2–3 V to be reached with this design.

The objective of this work was to fabricate an economical design of a 2 V DLC power supercapacitor in a total volume of 100 cm^{-3}. The capacitance of the cell was planned to be close to 300 F, leading to a volumetric capacitance of 25 F cm^{-3} per electrode, and to have a time constant between 2 and 3 s.

2. Experimental

2.1. Electrodes

Norit SX Ultra activated carbon (1200 m^2 g^{-1}, 8 F g^{-1}) was used as the active material. An electronic conductor was added to the carbon in order to ensure good electronic conductivity. A mixture containing the active material and the electronic conductor was added to a solution of carboxymethylcellulose (CMC) in water, or into a solution of poly(tetrafluoroethylene) (PTFE) in water. The mixture was then spread out on two different

* Corresponding author

0378-7753/99/$ - see front matter
PII: S0378-7753(99)00069-5

current collectors: 2 mm thick nickel foam, 60 pores per inch (ppi) and 1.6 mm thick nickel foam of 110 ppi. After thermal treatment in air and then in vacuum, 4 cm^2 electrodes were assembled face-to-face, with a cellulosic separator in between, and introduced into a hermetically sealed cell. All the electrode compositions are listed in weight percent (wt.%). Cells were then filled with electrolyte, which was a solution of acetonitrile (ACN) containing 1.7 M of NEt_4MeSO_3. This electrolyte has a good conductivity (20 mS cm^{-1} at 25°C), and does not contain fluorine compounds.

The electrochemical impedance apparatus consisted of a Solartron Schlumberger 1255 frequency response analyzer and a 1286 electrochemical interface. The frequency range was 2 kHz–10 mHz.

2.2. Capacitance and resistance measurements

Prismatic cells 4 cm^2 were assembled with a cellulosic separator in between the electrodes. They were cycled 150 times at a constant current density of 10 mA cm^2 between 0 and 2 V using Bitrode (time resolution: 1 s) and Biologic VMP (time resolution: 20 ms) equipments. The characteristics of the supercapacitors remained constant during these cycles. Capacitance was calculated from the slope of the $V(t)$ plot. Resistance measurements were made using an Solartron Schlumberger 1255 electrochemical impedance spectrometer (at 1000 Hz), or were calculated from the ohmic drop during cycling with the VMP apparatus. The resistivity of the cells was calculated from:

$$\rho = R \times S/t$$

where S is the surface area of the cell, t the thickness and R the resistance of the cell measured during cycling.

3. Results and discussion

3.1. Electrode composition

3.1.1. PTFE-based electrodes

This part of the work presents the results obtained from different electrode compositions. The objective was to increase the activated carbon content, while keeping good mechanical properties and low resistivity of the electrodes. Tests were carried out on two-electrode.

Cells 4 cm^2 in size were assembled with different electrode compositions. A constant pressure was applied to the cell, and six cellulosic separators were placed between the electrodes to avoid short-circuits. All the electrodes were pasted with 0.4 g cm^{-3} ($\pm$20 mg) of active material. The thickness of the electrodes was between 650 and 750 μm. The starting electrode composition was defined on the basis of previous results [8]: 80% activated carbon, 15% carbon graphite, 5% CMC, abbreviated to: 80% AC/15% CG/5% CMC. This composition was found to confer a good level of conductivity associated with a volumetric capacitance of more than 15 F cm^{-3} of electrode. It was noted that an activated carbon content higher than 80% greatly decreased the mechanical properties of the electrodes.

Preliminary experiments were carried out using PTFE as binder to try and increase the activated carbon content in the electrodes. Different compositions were tested: 90% AC/5% CG/5% PTFE; 95% AC/5% PTFE; 97% AC/3% PTFE and 98% AC/2% PTFE. The mechanical properties of the electrodes were much improved, when compared to the CMC ones. This can be attributed to the differences existing in the PFTE and CMC binding action. The CMC binds small amounts of active material and the PTFE makes active material fibrils strongly adherent among themselves. Table 1 presents the resistivity of the cells with these different electrode compositions (the high values of the resistivity come from the contribution of the thick separator needed to avoid short circuits in these types of experiments). For the electrodes containing 5% binder (PTFE or CMC), it can be seen that the resistivity of the cells is the same. The use of PTFE allowed an increase in the activated carbon content in the electrode without changing the resistivity. But the increase of the activated carbon/PTFE ratio from 95/5 to 98/2 led to the increase in resistivity, especially for the cells using electrodes made of 97% AC, 3% PTFE and 98% AC, 2% PTFE. The adherence of the active material on the current collector was very poor for these latter two compositions, making them impractical for electrode manufacturing.

Fig. 1 presents the impedance spectra of the cells containing PTFE-based electrodes with the following compositions: 90% AC/5% CG/5% PTFE; 95% AC/5% PTFE; 97% AC/3% PTFE and 98% AC 12% PTFE. It can be seen that the shape of the plots is similar for all the cells over the frequency range studied (2 kHz–10 mHz).

Table 1
Resistivity of various binder/carbon active materials

Composition (percentage AC/percentage CG/ percentage binder)	Mass (mg cm^{-3})	Resistivity (Ω cm)
80/15/5 CMC	0.41	44
90/5/5 PTFE	0.41	43
95/0/5 PTFE	0.40	46.4
97/0/3 PTFE	0.38	50.8
98/0/2 PTFE	0.4	60

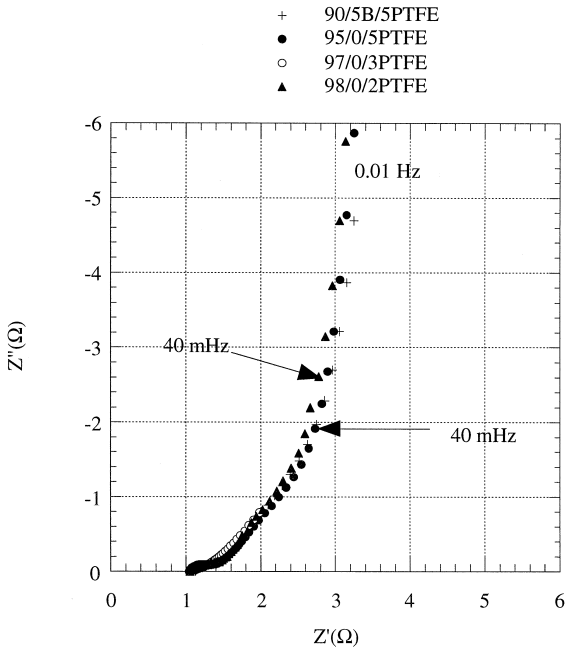

Fig. 1. Impedance spectra between 2 kHz and 10 mHz of cells containing PTFE-based elctrodes.

The knee frequency, which is not very sharp, appears at 40 mHz. This frequency separates two different phenomena in the cell: above this frequency, the frequency-dependence of the real part of the impedance (R) shows electrolyte penetration into the porous structure of the electrode. Below this frequency, the impedance of the cell increases and tends to become purely capacitive. The same behaviour is observed for all of the cells in this frequency domain. It can then be concluded that these PTFE-based electrodes did not present important differences in their frequency behaviour.

3.1.2. CMC / PTFE-based electrodes

Electrodes were prepared using a mixture of the two binders PTFE and CMC. By modifying the fabrication process, it has been possible to make electrodes containing 5% of mixed binders. Two different CMC/PTFE-based electrodes were prepared, with different binder compositions. In the rest of the paper, these two compositions will be called binder a and binder b. For each, the total content of the binder is 5%.

In order to improve the electrode composition, different graphites were also tested:

(a) a disk-shaped graphite called GMP, from the Université de Nancy,

(b) a 44 μm spherically-shaped graphite called SFG44, from LONZA,

(c) 6 μm diameter graphite fibres.

From previous observations, which had shown a decrease in the mechanical properties of the electrodes, the activated carbon content in these experiments never exceeded 90%. It is important to note that the electrodes bound with PTFE/CMC mixtures exhibited mechanical properties greatly improved over the CMC ones.

Table 2
Resistivity of cells containing electrodes using different graphites and binders

CG type	Resistivity (Ω cm)		
	90% activated carbon plus 5% CG plus:		
	5% PTFE	5% Binder a	5% Binder b
GMP	44.5	39.5	36.5
SFG44	43.0	35.0	29.0
Fibres	42.2	41.5	41.1

At first, electrodes containing 90% AC/5% CG/5% binder were prepared. The three graphites were tested, as well as the binder mixtures a and b. Table 2 presents the results obtained from 4 cm^2 cells, assembled with such electrodes.

The first point to note is the change in the resistivity with the nature of the binder: whatever the graphite used, the lower resistivities were measured with compositions containing binder b. Then, it can be observed that the electrodes made of SFG44 graphite gave the lowest resistivity values. The best electrode composition was found to be: 90% AC/5% CG (SFG44)/5% binder b, so the use of SFG44 associated with CMC/PTFE binder mixtures seemed to be suitable for electrode fabrication.

Fig. 2 presents the impedance spectra of cells containing electrodes made of 90% AC/5% GMP/5% binder. The knee frequency appears at 25 mHz, a low value which can be explained by the thickness of the separators. An

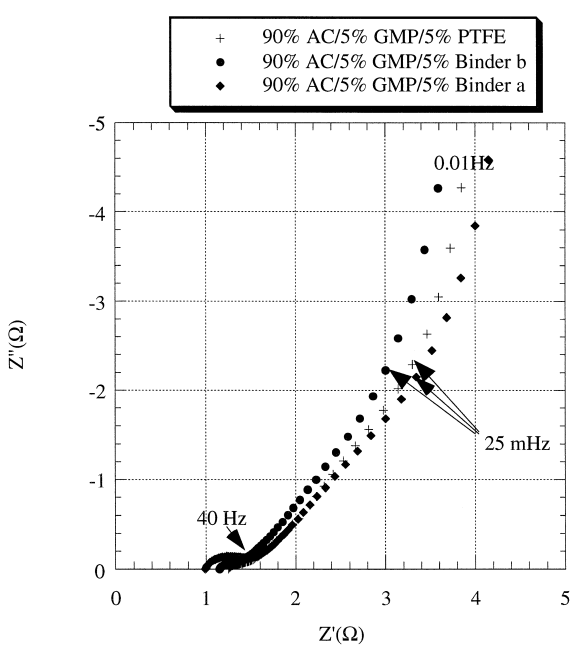

Fig. 2. Impedance spectra between 2 kHz and 10 mHz of cells containing electrodes made from 90% activated carbon, 5% carbon graphite, and 5% of different types of binder.

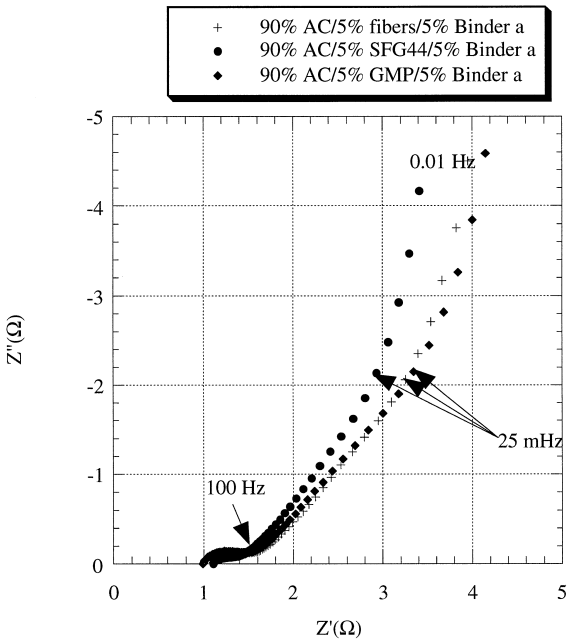

Fig. 3. Impedance spectra between 2 kHz and 10 mHz of cells containing electrodes made from 90% activated carbon, 5% of different graphites and 5% of binder 'a'.

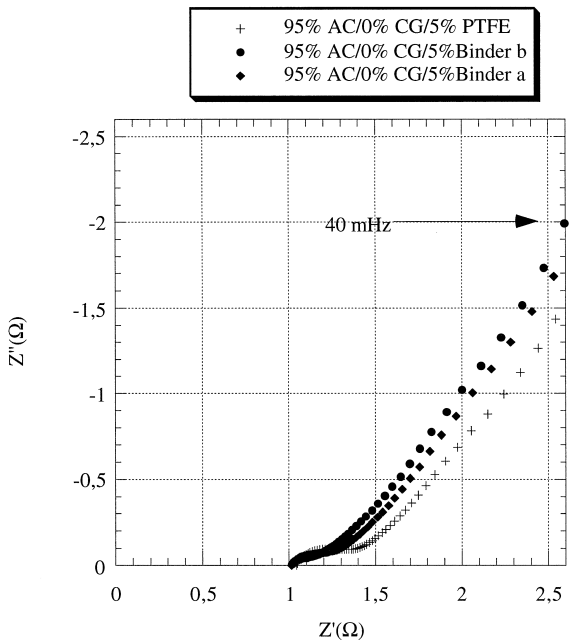

Fig. 4. Impedance spectra between 2 kHz and 10 mHz of cells containing electrodes made from 95% activated carbon, no graphite, and 5% of different types of binder.

interesting point concerns the slope of the plot below the knee frequency. This part of the spectrum is related to electrolyte penetration into the porous structure of the electrode. The increases of the $(\Delta Z'')/(\Delta Z')$ slope shows an improvement of the electrolyte penetration into the electrode. Binder a- and PTFE-based electrodes exhibit the same behaviour, with similar slopes. The last composition (90% AC/5% GMP/5% binder b) presents an increase of the slope as compared to the others. With this composition, the electrolyte penetration is slightly improved, which leads to the decrease of the frequency dependence of the real part of the resistance. Similar results were obtained whatever was the nature of the graphite.

Fig. 3 represents the impedance spectra of the cells containing electrodes made of 90% AC/5% CG/5% binder a. The three different graphites were tested. It can be seen that the knee frequency appears at 25 mHz. Above this value, the frequency dependence of the resistance is decreased for that of 90% AC/5% SFG 44/5% binder 'a' composition. This behaviour, associated with the slight increase of the $(\Delta Z'')/(\Delta Z')$ slope shows that the electrolyte penetration into the pores of the electrode is slightly increased when the composition contains 5% SFG44, irrespective of the nature of the binder.

Table 3
Resistivity of cells containing 95% activated carbon and 5% binder

Type of binder	Mass (g cm^{-3})	Resistivity (Ω cm)
PTFE	0.4	46.3
Binder 'a'	0.42	44.0
Binder 'b'	0.4	37.0

In order to increase the activated carbon content in the electrodes, 4 cm^2 cells containing electrodes made of 95% AC/0% CG/5% binder were assembled and tested. Table 3 lists the characteristics measured for these cells. Once again, best results were obtained with binder 'b', where the lowest value of the resistivity was measured. This decrease can be explained by an improvement of the active material/current collector adherence when binder 'b' is used, as the mechanical properties of such electrodes are improved.

Fig. 4 presents the impedance spectra of the cells enlarged between 2 kHz and 40 mHz, the frequency range where the electrolyte penetration into the porosity of the electrode can be seen. The use of two binder mixtures 'a' and 'b' led to an improvement of the electrolyte penetration, as it is shown in Fig. 4. The real part of the

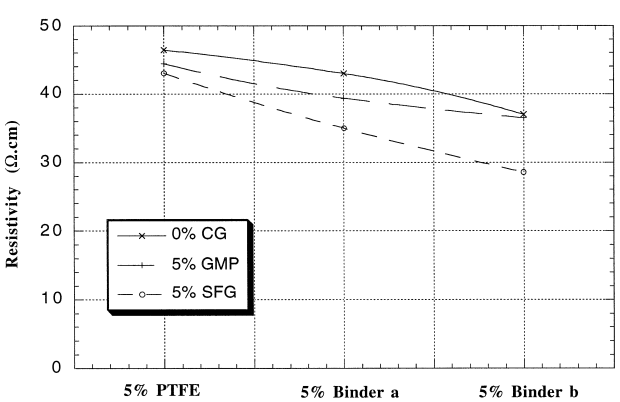

Fig. 5. Variation in the resistivity of cells with 5% of different binders and 5% or no graphite.

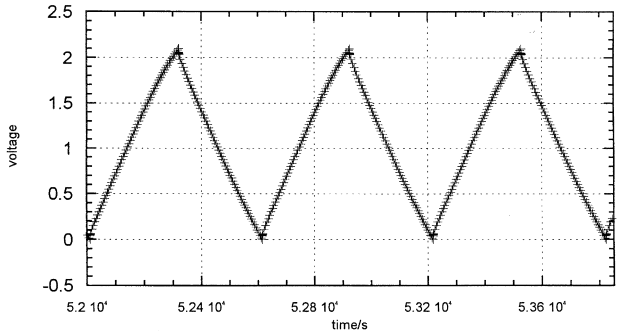

Fig. 6. Charge–discharge galvanostatic cycling at 2 A, 25°C of the supercapacitor.

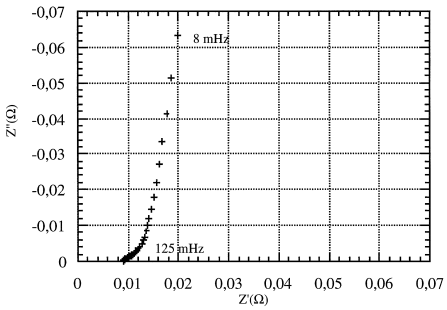

Fig. 7. Impedance spectrum between 2 kHz and 10 mHz of the supercapacitor.

impedance (the resistance) is less frequency dependent for these two compositions. Here again, cells containing electrodes made of binder 'b' exhibit the best behaviour. The use of the PTFE/CMC mixtures allowed us to increase the activated carbon content in the electrode, also the mechanical properties were much increased.

Fig. 5 plots the resistivity of the cells against composition of those electrodes which contained 5% and 0% of graphite. From these curves, it appears that the best binder is the 'b' mixture of PTFE/CMC, and the lowest resistivity values were obtained with a SFG44 graphite content of 5% in the electrode. The electrode composition which gave the most interesting results was: 90% activated carbon/5% SFG44/5% binder 'b' (PTFE/CMC).

This study of the electrode composition has shown that the use of PTFE/CMC binder mixtures could improve the performances of the electrodes, as compared to the use of pure CMC [8]. The activated carbon content in the electrode can be increased (up to 90 or 95%), and the mechanical properties of the electrodes are improved. The frequency dependence of the cell's resistance is not as strong as for pure PTFE-based electrodes.

4. Supercapacitor tests

In this section, a prismatic supercapacitor containing large electrodes was assembled and tested in order to verify the previous results obtained on small laboratory cells. A supercapacitor containing 26 electrodes each 31.5 cm^2 was assembled. The thickness of the electrodes was 600 μm. Two sets of 13 parallel-connected electrodes were used. They were made from the CMC/PTFE binder, but with no graphite. so that the activated carbon content in the electrode could be maximised. The composition was: 95% AC/0% CG/5% binder 'b'. A 150 μm cellulosic separator was placed between the electrodes. The inner dimensions of the case were $45 \times 85 \times 18$ mm^3.

4.1. Constant current cycling

Fig. 6 presents galvanostatic charge–discharge cycling at 2 A. It can be seen that no faradaic processes occur in the potential range studied (0–2.15 V). Table 4 lists the supercapacitor characteristics measured during cycling at 2, 4, and 10 A at 25°C. The low current test (2 A) on the supercapacitor was performed on a Biologic VMP which is a multi-channel battery tester. The VMP tester is capable of measuring voltage differences of a fraction of a millivolt, and takes data at rates of up to 50 Hz, which was particularly useful in determining the resistance of the cell.

The capacitance was found to be 350 F at 2 A. This leads to a specific capacitance of 75 F g^{-1} of activated carbon, which is close to the theoretical specific capacitance value of Norit SX Ultra (80 F g^{-1}). It can therefore be concluded that all the activated carbon is acting capacitively. The volumetric capacitance is 27 F cm^{-3} per electrode (including the current collector). This value equates to the defined objective of 25 F cm^{-3} per electrode. The planar resistance, calculated from the value of R, is 7 Ω cm^{-2}, rather higher than the desired one of 5 cm^{-2}. The values of the resistance and the capacitance lead to a specific power of 1 kW kg^{-1} and a specific energy value of 1.7 W h kg^{-1} (both values are based on the total weight of the supercapacitor). The time constant of the cell is 3.1 s, and this value makes it compatible with starting applications.

Table 4
Electrical characteristics obtained when the supercapacitor was discharged at 2, 4, and 10 A at 25°C

Current (A)	Initial voltage (V)	Capacitance (F)	Resistance (mΩ)	Maximum specific power (kW kg^{-1})	Maximum specific energy (W h kg^{-1})
2	2.10	348	9	1	1.6
4	2.10	351	8.2	1	1.6
10	2.11	347	7.5	1	1.6

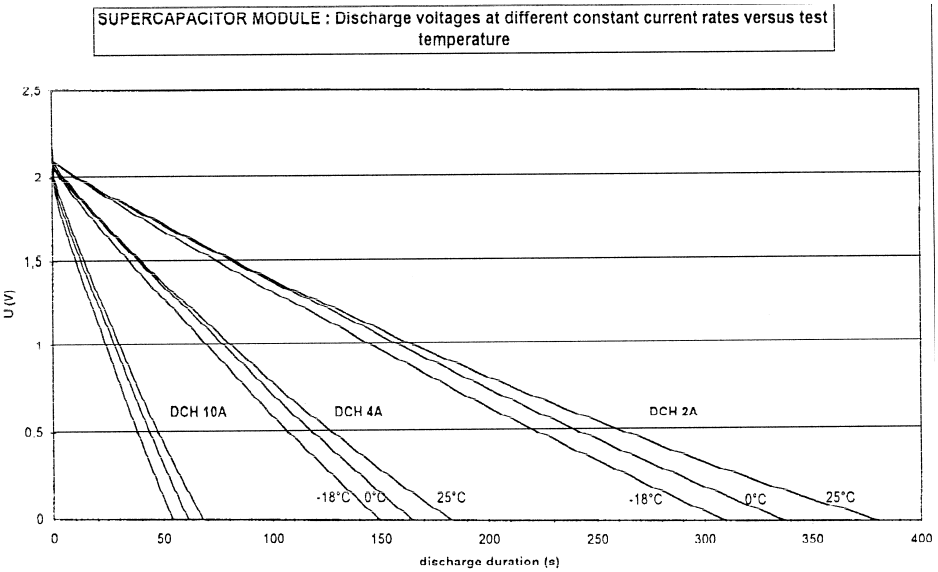

Fig. 8. Voltages against time-into-discharge of the supercapacitor, at various currents (2, 4, and 10 A) and temperatures (−18, 0, and +25°C).

4.2. Impedance measurements

Fig. 7 presents the impedance spectrum of the supercapacitor between 2 kHz and 8 mHz. The knee frequency appears at 125 mHz, which is a correct value. The behaviour of the supercapacitor below this frequency tends to be the one of a pure capacitance, as the impedance is close to the vertical line. The real part of the impedance is not strongly frequency-dependent: there is a factor of 2:1 between the low frequency value of the resistance (8 mHz) and the high frequency value (2 kHz). Electrolyte penetration is easily achieved and the electrodes are active throughout their full volume.

4.3. Low temperature cycling

Fig. 8 presents the cycling of the supercapacitor at different temperatures and currents, and Table 5 lists the characteristics measured during cycling. The temperature range was +25 to −18°C, the currents 2, 4 and 10 A. When temperature was changed from +25 to −18°C, the capacity loss of the cell was 18%, to a rather low value. The loss of maximum specific energy was 12% over the same range of temperature.

An interesting point concerning the change in resistance with respect to the temperature from 25 to −18°C is that the resistance is multiplied by a factor of 1.3, giving a specific power loss of 28%. These characteristics make the supercapacitor useful for operating at low temperatures. However, the resistance of the cell must be decreased in order to reach a planar resistance of 5 $m\Omega\ cm^{-2}$.

This should be possible by using electrodes composed of: 90% activated carbon/5% SFG44/5% binder 'b' (PTFE/CMC), as previous results have shown that cells containing such electrodes gave the lowest resistivity. These results will be presented in a future paper.

Table 5
Electrical characterisitics obtained when the supercapacitor was discharged at 2, 4, and 10 A at 25°, 0, and −18°C

Temperature (°C)	Current (A)	Initial voltage (V)	Capacitance (F)	Resistance (mΩ)	Maximum specific power (kW kg^{-1})	Maximum specific energy (W h kg^{-1})
25	2	2.10	348	8.2	1	1.6
	4	2.10	351	8.2	1	1.6
	10	2.11	347	8.2	1	1.6
0	2	2.13	320	10.1	0.83	1.5
	4	2.13	321	10.1	0.83	1.5
	10	2.13	318	10.1	0.83	1.5
−18	2	2.14	293	11.8	0.72	1.4
	4	2.14	293	11.8	0.72	1.4
	10	2.14	288	11.8	0.72	1.4

5. Conclusions

This study focused on the electrode composition for carbon/carbon power supercapacitor. In the first part of this paper, it was shown that electrode performances were improved by using a mixture of two binders, PTFE and CMC.

Laboratory cells containing such electrodes exhibited lower values of resistivity and the mechanical properties of the electrodes were improved. Best results were obtained with the following electrode composition: 90% activated carbon/5% SFG44/5% binder 'b' (a mixture of PTFE and CMC). A supercapacitor containing large electrodes was then assembled with electrodes made of 95% activated carbon/5% binder 'b'. A maximum specific power of 1 kW kg^{-1} and a maximum specific energy of 1.6 W h kg^{-1} (based on the total weight of the cell) were reached at 25°C. When lowering the temperature from +25 to −18°C, the loss of maximum specific energy was 12% while the loss of maximum specific power was 28%. The time constant was 3.1 s, compatible with power applications. The volumetric capacitance of the cell was calculated as 27 F cm^{-3} per electrode (including current collector).

Future work will consist of decreasing the resistance of the supercapacitors, by using the following composition for the electrodes: 90% activated carbon/5% SFG44/5% binder 'b' (PTFE/CMC). First results have already shown a decrease in the resistance of the cells containing such electrodes, and the results will be published in a future paper.

Acknowledgements

The authors would like to thank the Ministère de I'Education Nationale, de la Recherche et de la Technologle, and the 'Délégation Générale pour I'Armement' for their financial support of this work.

References

[1] B.E. Conway, Fundamentals and applications of electrical capacitors, 188th Meeting of the Electrochem. Soc., Chicago, IL, 1995.
[2] J.R. Miller, Technical status of large electrical capacitors, Proc. 12th International Seminar on Battery Technology and Applications, Deerfield Beach, FL, 1995.
[3] J.P. Zheng, T.R. Jow, J. Electrochem. Soc. 142 (1995) L6.
[4] J.P. Ferraris, I.D. Brotherston, D.C. Loveday, Proc. 38th Power Sources Conference, Cherry Hill, NJ, 1998.
[5] J. Farahmandi, D. Gideon, Proc. 6th International Seminar on Double Layer Capacitors and Similar Energy Storage Devices, Deerfield Beach, FL, 1996.
[6] P. Konsweil, O. Scchmid, A. Loffier, Proc. 7th International Seminar on Double Layer Capacitors and Similar Energy Storage Devices, Deerfield Beach, FL, 1997.
[7] M.F. Rose, C. Johnson, T. Owen, B. Stephen, J. Power Sources 47 (1994) 303.
[8] L. Bonnefoi, P. Simon, J.F. Fauvarque, C. Sarrazin, A. Dugast, Proc. 38th Power Sources Conference, Cherry Hill, NJ, 1998.